ECS Transactions, 19 (6) 109-117 (2009)
10.1149/1.3118543 ©The Electrochemical Society

Waveguide-Based Chemical and Spectroelectrochemical Sensor Platforms

Brooke M. Beam,[a] Adam Simmonds,[a] P. Alex Veneman,[a] Erin Ratcliff,[a]
Sergio B. Mendes,[b] S. Scott Saavedra,[a] Neal R. Armstrong*[a]

[a]Department of Chemistry, University of Arizona, Tucson, Arizona 85721
[b]Department of Physics, University of Louisville, Louisville, Kentucky

Here we review the progress in the development of waveguide-based spectroelectrochemical platforms, with special emphasis on the most recent technologies: the electroactive fiber-optic chip (EA-FOC) and chip-like spectroelectrochemical platforms using organic light emitting diode (OLED) light sources coupled with organic photovoltaic photodetectors (OPV-PD). Both technologies simplify spectroelectrochemical data collection through eliminating the need for free-space optics and benefit from the increased sensitivity of waveguide based devices producing new chemical sensor platforms.

Introduction

Combining spectroelectrochemical sensor platforms with integrated optical waveguide sensors (Fig. 1) has been a goal of many research groups, dating back to the first transmission and attenuated total reflectance (ATR) spectroelectrochemical platforms (1-4). From the first spectroelectrochemical experiments, it was recognized that spectroscopic probes provide information about redox events at electrode surfaces without interference from the optically inactive charging current backgrounds. Additionally, high sensitivities were achieved by optimizing the pathlength of the optical platforms (Fig. 2), allowing investigation of even sub-monolayer coverages of electrochemically active species. Spectroelectrochemical platforms have subsequently been utilized to measure rates of heterogeneous electron transfer for solution soluble species, and rates of electron transfer (ET) for surface-confined molecules and conducting polymers (5-19) as well as for various analyte sensing studies (20-24). Initial studies were confined to visible light, however, spectroelectrochemical techniques now cover most of the electromagnetic spectrum, leading to a large variety of "hyphenated" electrochemical techniques. Our collective efforts began with the development of the most challenging spectroelectrochemical platform, coupling visible light into step-index single-mode waveguides which were overcoated with transparent conducting oxides such as indium-tin oxide (ITO) (Fig. 1A) (7, 8). This work closely followed the work of Fujishima and coworkers who had demonstrated the spectroelectrochemical properties of gradient index channel waveguides overcoated with an electroactive tin oxide (ATO) layer (5). The electroactive integrated optic waveguide (EA-IOW) provided the highest sensitivity yet produced for the spectroelectrochemical characterization of redox events for surface confined molecules such as methylene blue (MB), with sensitivity enhancements compared to transmission spectroelectrochemical experiments of 10^3x up to 10^4 x (Fig. 1a). As an extension of studies using achromatic prism/grating couplers to extend the spectral coverage of single-mode IOWs (26, 27), the initial EA-IOW design was then modified to use achromatic prism couplers which provided for coupling most of the visible wavelength region into the single-mode EA-IOW (Fig. 1b). The increased

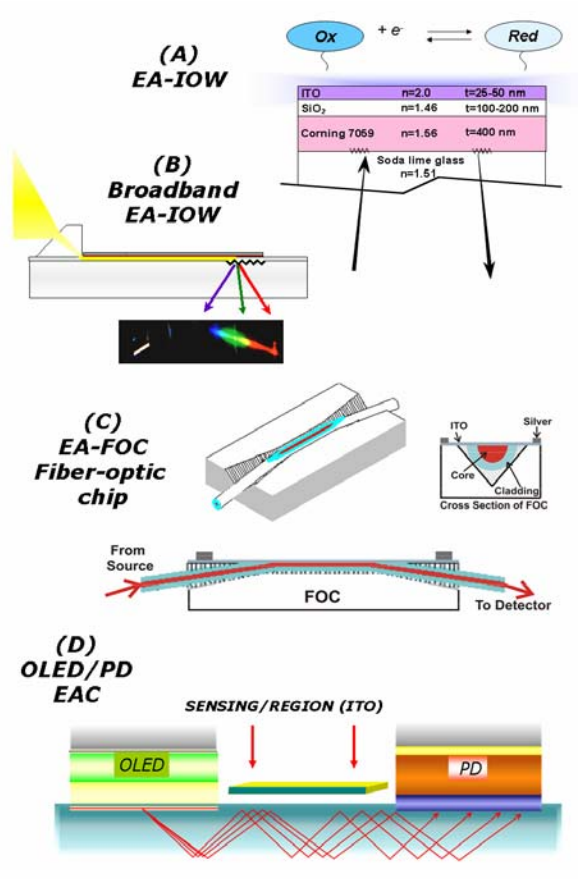

Figure 1. Schematic views of waveguide/ATR-based spectroelectrochemical platforms. (A) The electroactive integrated optical waveguide, where an indium-tin oxide electrode coats a single mode waveguide, providing for an enhancement in spectroelectrochemical sensitivity of ca. 10,000x; (B) The broadband EA-IOW, where prism coupling of white light into a single mode EA-IOW provides for spectroelectrochemical sensing across the full visible wavelength region; (C) an electroactive, side-polished fiber optic chip (EA-FOC), where polishing provides a flat surface overcoated with the electroactive layer – this technology provides for ease of broadband coupling of white light sources, and out-coupling to multichannel detectors; (D) a platform coupling the light output of an organic light emitting diode (OLED) into ATR modes, with detection via an organic photodetector (OPV-PD) assembly – an electroactive region between the OLED and PD provides for spectroelectrochemical characterization of a surface confined redox couple.

optical pathlength (Fig. 2) of a single mode waveguide, capable of broadband spectroscopy with simultaneous electrochemical control, produced unprecedented sensitivities in simple spectro-electrochemical measurements (9, 11, 13). These platforms, however, are not straightforward to produce, and require special alignment of the laser or broadband source, using grating in-coupling and out-coupling of the light. Therefore the EA-IOW is somewhat difficult to produce in rugged field-portable platforms.

Later versions of the EA-IOW platform returned to thin ATR elements, which are easier to implement, exhibiting ca. 10-150x sensitivity enhancement over a transmission experiment (Fig. 2) (10, 16). However, these ATR platforms exhibit sufficient sensitivity to interrogate conducting polymer thin films on the ITO surface, and provide for ease of coupling of broadband visible light into the ATR element and using multi-channel detection (10, 14, 17, 25).

In all of these cases there was still a clear need for simplifying the EA-IOW platform to provide for field-portability and multi-channel detection in an easier to implement device platform. This need provided the motivation for the two new device platforms described here: 1) The electro-active fiber-optic chip (EA-FOC) (28, 29) and; 2) an electroactive ATR element using an organic light emitting light source (OLED) and an organic photovoltaic photodetector (OPV-PD)– the electroactive OLED/OPV spectro-

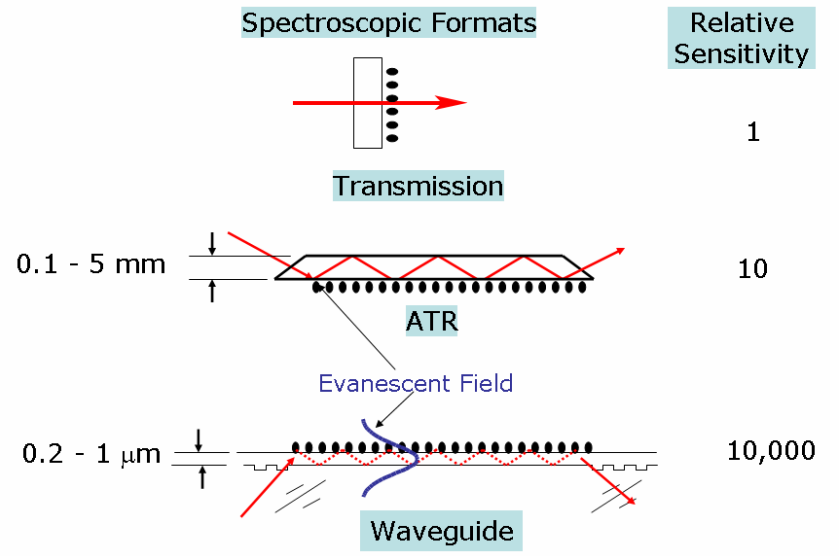

Figure 2. Schematic views of transmission mode spectroelectrochemistry, and the internal reflection modes for ATR and waveguide-based spectroelectrochemical platforms. As the thickness of the ATR element decreases the number of internal reflections per unit sensor length increases (or optical pathlength), as does the spectroscopic sensitivity. As the dimensions of the ATR element approach the wavelength of light, the propagation of electromagnetic radiation is best described by variations on Maxwell's equations, taking into account the refractive indices of the waveguide, the adsorbed molecular layers, and the superstrate (solution) (13).

electrochemical platform (EA-OOC) (30). Both of these platforms push spectro-electrochemical sensing into new regimes of portability, wide dissemination, and low-cost.

The Electroactive Fiber Optic Chip (EA-FOC)

Fig. 1C shows a schematic view of the EA-FOC. The fiber-optic chip platform (FOC) consists of a multi-mode optical fiber embedded in a V-groove "chip." Side-polishing of the fiber, sufficient to expose a portion of the core region, provides for a waveguide-like sensing platform. The sensing region dimensions are determined by the type of optical fiber, the V-groove dimensions, and the polishing protocols. The planar, chip-like format of the FOC provides for broadband excitation via standard fiber coupling protocols and connection to standard multichannel detectors. Full visible wavelength spectroscopic information is obtainable in a straightforward manner, without the need for free-space optics (prism and/or grating couplers) which make normal waveguide sensors more difficult to export to applications requiring field-portability (28). To impart electroactivity, the FOC is coated with an indium-tin oxide (ITO) thin film as the working electrode, and the EA-FOC is sealed in a conventional three-electrode electrochemical cell.

Our first EA-FOC experiments focused on probing electrochemically driven changes in absorbance for the reduction of surface-confined methylene blue to it leuco form. This redox probe is convenient to explore in aqueous environments, and it has been used in

several previous electroactive waveguide spectroelectrochemistry experiments, providing for a direct comparison of sensitivities across all of these sensing platforms (5, 7). For the EA-FOC, we found a sensitivity enhancement of ca. 40x versus a transmission measurement, which compares with a sensitivity enhancement for electroactive channel waveguides of ca. 150x (5) and for single-mode EA-IOWs of ca. 10,000x (7). Even with a lower sensitivity enhancement, the EA-FOC can probe the redox spectroelctrochemistry of extremely low coverages of electrodeposited conducting polymer thin films, i.e. about 0.3 % of a monolayer of poly(3,4-ethylenedioxythiophene) (PEDOT) (29). There is clearly a compromise in sensitivity for the EA-FOC, in these first generation platforms, which is offset by their increased ease of use. The next-generations of this technology will address increasing the sensitivity enhancement, and it is likely that these platforms will begin to compete with certain multi-mode waveguides in certain sensing applications.

The Electroactive OLED/OPV Chip (EA-OOC)

Our most recent efforts have been to produce a spectroscopic sensing platform with a fully integrated light source and detector (EA-OOC) (Fig. 1d). The EA-OOC spectroelectrochemical platform uses a thin film organic light emitting diode (OLED) light source, coupled on an ATR element with an organic photovoltaic photodetector (OPV-PD) (Fig. 1d). Thin film light sources have been developed over the last twenty years, based on vacuum-deposited small molecules (OLED), or spin-cast or printed polymers (the polymer light emitting diode, PLED), which can be used as excitation sources for sensing platforms (32-46). Using OLEDs or PLEDs as thin film light sources in transmission geometries is straightforward, and produces compelling sensor platforms (35, 39, 42, 47, 48). It is well known, however, that the forward emission (in the display direction) of conventional OLEDs or PLEDs constitutes not more than ca. 20% of their emission, with the bulk of that emission captured in “waveguide modes” within the organic layers, or “substrate modes” (attenuated total internal reflectance) within the glass or plastic substrate materials (54-62). Emission at or above the critical angle for internal reflection in the substrate is captured in ATR modes within the substrate and used to integrate a thin film sample deposited on the glass slide (54-62). The number of internal reflections before striking the detector is controlled by the thickness of the substrate (Fig. 2), the refractive indices of organic, ITO and substrate layers, and the length of the sensing region.

For our first-generation EA-OOC devices, we have used simple two-layer OLED light sources, based on the green (and broad) emission from aluminum quinolate (49, 50), integrated on the same chip with conventional OPV-PDs, based on copper phthalocyanine/fullerene ($CuPc/C_{60}$) heterojunctions (51-53). The power conversion efficiencies of our first-generation OPV-PDs, are typically in the range of 1-2 % under AM1.5 illumination conditions (52, 63-65), however, this is typically adequate sensitivity for use in these EA-OOC sensor platforms. We have modeled the input and output coupling of OLED emission into ATR modes and then collection by the OPV-PD using a ray optics approach (combinations of Snell’s Law and the Fresnel relationships to describe internal reflection and refraction). The modeling calculations predict that greater than ca. 8% of OLED emission is detected by the OPV-PD, in the absence of changes in refractive index of the superstrate solution (66). Using this platform we have been able to

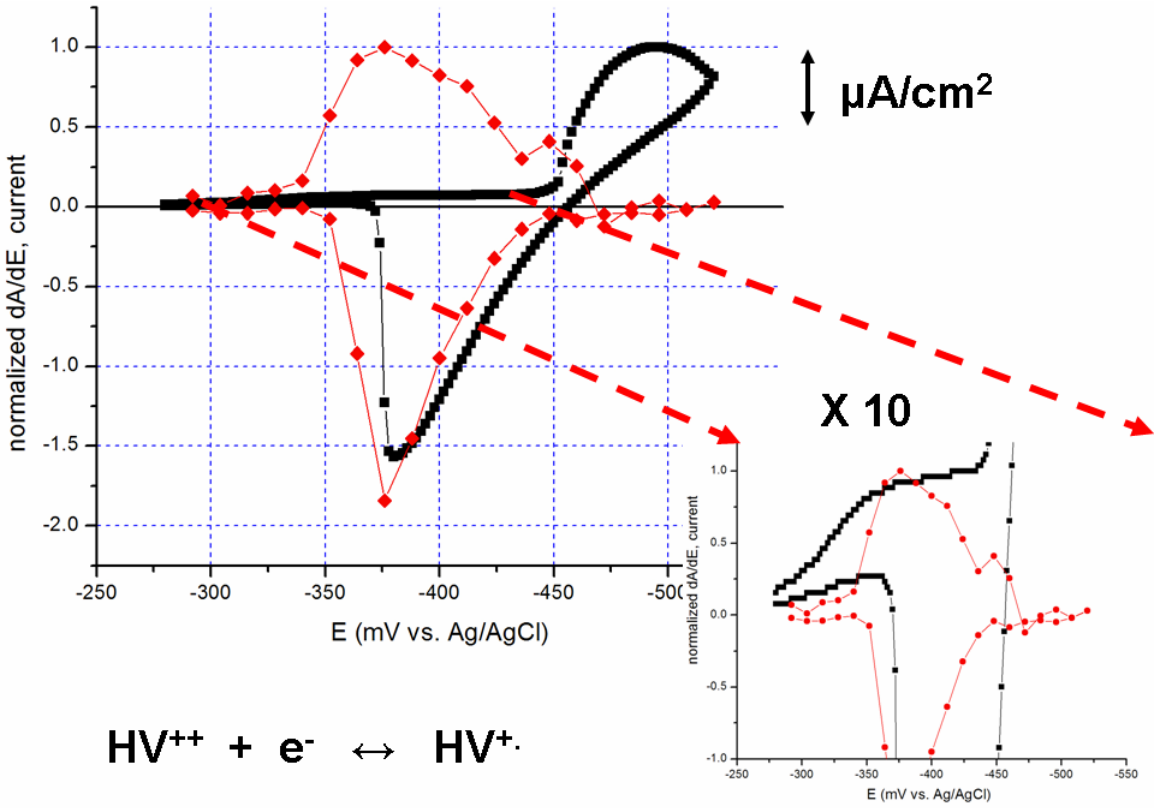

Figure 3. Voltammetric (black points) and absorptovoltammetric response (red points) of the EA-OOC to the reduction of n-heptylviologen (n-HV^{++} +e^- → n-$HV^{+\cdot}$). The voltammetric response is as expected, with mass transport controlled reduction of n-HV^{++} to n-$HV^{+\cdot}$, followed by stripping of the surface confined reduction product during sweeps to positive potentials. The absorptovoltammetric response (ΔA/ΔV) actually shows its most significant change in a potential region before the mass transport reduction, corresponding to underpotential deposition of the first monolayer of the reduction product and tracks the changes in absorbance occurring during the stripping step.

detect changes in refractive index of a series of superstrate solutions in the sensing region down to levels of ca. +/- 0.005 units (66).

Placing an electronically isolated ITO electrode in the sensing region provides for simple spectroelectrochemical sensing, and for this first-generation application we chose a simple redox system, the one-electron reduction of n-heptyviologen to its surface confined (deeply colored) cation radical state (n-HV^{++} + e^- → n-$HV^{+\cdot}$) (67-70). The absorbance changes of n-heptyviologen during the electrochemical process reasonably match the output emission of our aluminum quinolate OLED excitation source (Fig. 3). Both current-voltage and changes in absorbance versus changes in potential (ΔA/ΔV) data are shown. In theory, these data should track each other, however, as can be seen in the reduction sweep in Fig. 3, a significant change in ΔA/ΔV at potentials positive of the onset of mass transport controlled reduction of n-HV^{++} is observed. This change in ΔA/ΔV is consistent with underpotential reduction of a pre-adsorbed layer of n-HV^{++}, which produces a significant change in effective refractive index at the electrode/solution

interface (67). Expanding the sensitivity in the voltammetric experiment confirms that a "pre-wave" is indeed seen in the voltammetric data, in this potential region (inset of Fig. 3), and that our EA-OOC is extremely sensitive to small refractive index changes associated with adsorption and reaction of such redox couples. Work now in progress extends the sensitivity of the OOC sensing platform even further through the use of a true dual-beam device platform, with a single OLED excitation source and multiple OPV-PDs, modulated operation of the OLED, and phase-locked detection modes (44).

Conclusions

It is clear that there is a strong future for optical and spectroelectrochemical sensing platforms, which take advantage of established and emerging technologies, providing for unique ways of using light to interrogate interfacial electrochemical processes. The EA-FOC has evolved out of the now common use of side-polished optical fibers in telecommunication devices and potentially gives many of the same advantages of planar waveguides, which can easily support thin films, especially for bio-sensing problems. The possibility of using common light sources, and readily available multi-channel detectors makes it likely that the EA-FOC will see application in a number of sensing problems, where single- or multi-mode waveguides requiring free-space optics, would be problematic. The EA-OOC provides even further advantages for certain sensing applications, where miniaturization of sensor platforms is key. In this case, we anticipate being able to use very inexpensive ATR and waveguide elements with the possibility of integrating these devices with on-chip signal processing, portable power generation, and RF-telemetry of the analytical results to a control node for a network of portable sensors. Both the EA-FOC and EA-OOC will increase spectroelectrochemical sensor applications where increased sensitivity, portability, and low cost are essential.

Acknowledgements

This research has been supported by a combination of grants from the National Science Foundation (CHE-0517963 (NRA), CHE-0518702 (SSS) and DBI-0352449 (SRM), the Science and Technology Center, Materials and Devices for Information Technology Research (NSF-DMR-0120967, and the National Institutes of Health R01EB007047.

References

1. T. Kuwana, R. K. Darlington and D. W. Leedy, *Anal. Chem.*, **36**, 2023 (1964).
2. N. Winograd and T. Kuwana, *Anal. Chem.*, **43**, 252 (1971).
3. T. Kuwana and N. Winograd, in *Electroanalytical Chemistry*, A. Bard Editor, p. 1, Marcel Dekker, Inc., New York (1974).
4. W. R. Heineman, F. M. Hawkridge and H. N. Blount, in *Electroanalytical Chemistry*, A. Bard Editor, p. 1, Marcel Dekker, Inc., New York (1984).
5. K. Itoh and A. Fujishima, *J. Phys. Chem.*, **92**, 7043 (1988).
6. K. Itoh and A. Fujishima, in *Electrochemistry in Transition*, O. J. Murphy, S. Srinivasan and B. E. Conway Editors, p. 219, Plenum Press, New York (1992).

7. D. R. Dunphy, S. B. Mendes, S. S. Saavedra and N. R. Armstrong, *Anal. Chem.*, **69**, 3086 (1997).
8. D. R. Dunphy, S. B. Mendes, S. S. Saavedra and N. R. Armstrong, in *Interfacial Electrochemistry: Theory, Experiment and Applications*, A. Wieckowski Editor, p. 513, Marcel Dekker, Inc., New York (1999).
9. J. T. Bradshaw, S. B. Mendes and S. S. Saavedra, *Anal. Chem.*, **74**, 1751 (2002).
10. W. J. Doherty, C. L. Donley, N. R. Armstrong and S. S. Saavedra, *Appl. Spectrosc.*, **56**, 920 (2002).
11. J. T. Bradshaw, S. B. Mendes, N. R. Armstrong and S. S. Saavedra, *Anal. Chem.*, **75**, 1080 (2003).
12. A. F. Runge and S. S. Saavedra, *Langmuir*, **19**, 9418 (2003).
13. J. T. Bradshaw, S. B. Mendes and S. S. Saavedra, *Anal. Chem.*, **77**, 28A (2005).
14. C. H. Ge, W. J. Doherty, S. B. Mendes, N. R. Armstrong and S. S. Saavedra, *Talanta*, **65**, 1126 (2005).
15. Z. O. Araci, Runge, A. F., Doherty, W. J., Saavedra, S. S., *Isr. J. of Chem.*, **46**, 249 (2006).
16. W. J. Doherty III, R. J. Wysocki, N. R. Armstrong and S. S. Saavedra, *J. Phys. Chem. B*, **110**, 4900 (2006).
17. T. W. McBee, L.-Y. Wang, C. Ge, B. M. Beam, A. L. Moore, D. Gust, T. A. Moore, N. R. Armstrong and S. S. Saavedra, *J. Am. Chem. Soc.*, **128**, 2184 (2006).
18. Z. O. Araci, A. F. Runge, W. J. Doherty and S. S. Saavedra, *J. Am. Chem. Soc.*, **130**, 1572 (2008).
19. S. M. Mendes, Saavedra, S.S., Armstrong, N.R., *Springer Series on Chemical Sensors and Biosensors* (in press).
20. S. E. Andria, J. N. Richardson, N. Kaval, I. Zudans, C. J. Seliskar and W. R. Heineman, *Anal. Chem.*, **76**, 3139 (2004).
21. T. Shtoyko, J. N. Richardson, C. J. Seliskar and W. R. Heineman, *Electrochim. Acta*, **50**, 3191 (2005).
22. S. D. Conklin, W. R. Heineman and C. J. Seliskar, *Electroanalysis*, **19**, 523 (2007).
23. C. M. Wansapura, C. J. Seliskar and W. R. Heineman, *Anal. Chem.*, **79**, 5594 (2007).
24. H. Kuramitz, A. Piruska, H. B. Halsall, C. J. Seliskar and W. R. Heineman, *Anal. Chem.*, **80**, 9642 (2008).
25. W. J. Doherty, R. J. Wysocki, N. R. Armstrong and S. S. Saavedra, *J. Phys. Chem. B*, **110**, 4900 (2006).
26. S. B. Mendes, L. Li, J. J. Burke, J. E. Lee, D. R. Dunphy and S. S. Saavedra, *Langmuir*, **12**, 3374 (1996).
27. S. B. Mendes, L. Li, J. Burke and S. S. Saavedra, *Opt. Commun.*, **136**, 320 (1997).
28. B. M. Beam, R. C. Shallcross, J. Jang, N. R. Armstrong and S. B. Mendes, *Appl. Spectrosc.*, **61**, 585 (2007).
29. B. M. Beam, N. R. Armstrong and S. B. Mendes, *Analyst,* (in press).
30. P. A. Veneman, B. Zacher, D. Huebner, A. Simmonds and N. R. Armstrong, in, B. Zhenan, M. Iain, S. Ruth and G. M. George Editors, p. Proc. SPIE (2008).
32. X. H. Wang, Hofmann, O., Das, R., Barrett, E. M., Demello, A. J., Demello, J. C., Bradley, D. D. C., *Lab Chip*, **7**, 58 (2007).
33. O. Hofmann, Wang, X. H., , deMello, J. C., Bradley, D. D. C., deMello, A. J., *Lab Chip*, **5**, 863 (2005).
34. O. Hofmann, Miller, P., Sullivan, P., Jones, T. S., deMello, J. C., Bradley, D. D. C., deMello, A. J., *Sens. Actuators B*, **106**, 878 (2005).
35. J. Shinar and R. Shinar, *J. Phys. D-Applied Physics*, **41,** 133001/1-133001/26 (2008).

36. E. Kraker, Haase, A., Lamprecht, B., Jakopic, G., Konrad, C., Kostler, S., *Appl. Phys. Lett.,* **92,** 178 (2008).
37. E. C. Chen, Tseng, S. R., Ju, J. H., Yang, C. M., Meng, H. F., Horng, S. F., Shu, C. F., *Appl. Phys. Lett.*, **93,** 063304/1 (2008).
38. H. Tanaka, T. Yasuda, K. Fujita and T. Tsutsui, *Adv. Mat.*, **18**, 2230 (2006).
39. R. Shinar, Zhou, Z. Q., Choudhury, B.,. Shinar, J., *Anal. Chim. Acta*, **568**, 190 (2006).
40. R. Shinar, Ghosh, D., Choudhury, B. Noack, M., Dalal, V. L., Shinar, J., *J. Non-Cryst. Solids*, **352**, 1995 (2006).
41. L. Burgi, Pfeiffer, R., Mucklich, M., Metzler, P., Kiy, M., Winnewisser, C., *Org. Electron.*, **7**, 114 (2006).
42. B. Choudhury, R. Shinar and J. Shinar, *J. Appl. Phys.*, **96**, 2949 (2004).
43. V. Savvate'ev, Chen-Esterlit, Z., Aylott, J. W., Choudhury, B., Kim, C. H., Zou, L., Friedl, J. H., Shinar, R., Shinar, J., Kopelman, R., *Appl. Phys. Lett.*, **81**, 4652 (2002).
44. P. A. Veneman, Zacher, B., Huebner, D., Ratcliff, E., Simmonds, A., Saavedra, S. S., Armstrong, N.R., (manuscript in preparation).
45. A. Pais, Banerjee, A., Klotzkin, D., Papautsky, I., *Lab Chip*, **8**, 794 (2008).
46. M. C. Gather, F. Ventsch and K. Meerholz, *Adv. Mat.*, **20**, 1966 (2008).
47. R. Shinar, Z. Q. Zhou, B. Choudhury and J. Shinar, *Anal. Chim. Acta*, **568**, 190 (2006).
48. R. Shinar, D. Ghosh, B. Choudhury, M. Noack, V. L. Dalal and J. Shinar, *J. Non-Cryst. Solids*, **352**, 1995 (2006).
49. C. W. Tang and S. A. Vanslyke, *Appl. Phys. Lett.*, **51**, 913 (1987).
50. S. E. Shaheen, G. E. Jabbour, B. Kippelen, N. Peyghambarian, J. D. Anderson, S. R. Marder, N. R. Armstrong, E. Bellmann and R. H. Grubbs, *Appl. Phys. Lett.*, **74**, 3212 (1999).
51. P. Peumans, A. Yakimov and S. R. Forrest, *J. Appl. Phys.*, **93**, 3693 (2003).
52. M. Brumbach, D. Placencia and N. R. Armstrong, *J. Phys. Chem. C*, **112**, 3142 (2008).
53. N. R. Armstrong, Carter, C., Donley, C., Simmonds, A., Lee, P., Brumbach, M., Kippelen, B., Domercq, B., Yoo, S. Y., *Thin Solid Films*, **445**, 342 (2003).
54. K. Neyts, *Appl. Surf. Sci.*, **244**, 517 (2005).
55. C. J. Lee, Pode, R. B., Moon, D. G.. Han, J. L.,. Park, N. H.. Baik, S. H., Ju, S. S., *Phys. Status Solidi A*, **201**, 1022 (2004).
56. F. S. Juang, Laih, L. H., Lin, C. J., Hsu, Y. J., *Jpn. J. Appl. Phys., Part 1*, **41**, 2787 (2002).
57. V. Bulovic, Khalfin, V. B., Gu, G., Burrows, P. E., Garbuzov, D. Z., Forrest, S. R., *Phys. Rev. B*, **58**, 3730 (1998).
58. R. H. Jordan, Rothberg, L. J., Dodabalapur, A., Slusher, R. E., *Appl. Phys. Lett.*, **69**, 1997 (1996).
59. J. M. Ziebarth and M. D. McGehee, *J. Appl. Phys.*, **97,** 064502/1 (2005).
60. D. Yokoyama, Nakanotani, H., Setoguchi, Y., Moriwake, M., Ohnishi, D., Yahiro, M., Adachi, C., *Jpn. J. Appl. Phys., Part 2*, **46**, L826 (2007).
61. L. H. Smith, J. A. E. Wasey, I. D. W. Samuel and W. L. Barnes, *Adv. Funct. Mater.*, **15**, 1839 (2005).
62. M. Cui, H. P. Urbach and D. K. G. de Boer, *Opt. Express*, **15**, 4398 (2007).
63. S. Yoo, Potscavage, W. J., Domercq, B., Han, S. H., Li, T. D., Jones, S. C., Szoszklewicz, R., Levi, D., Riedo, E., Marder, S. R., Kippelen, B., *Solid-State Electron.*, **51**, 1367 (2007).
64. S. Yoo, B. Domercq and B. Kippelen, *J. Appl. Phys.*, **97**, 9 (2005).

65. N. R. Armstrong, C. Carter, C. Donley, A. Simmonds, P. Lee, M. Brumbach, B. Kippelen, B. Domercq and S. Y. Yoo, *Thin Solid Films*, **445**, 342 (2003).
66. A. V. Simmonds, P. A., Zacher, B., Huebner, D., Ratcliff, E., Saavedra, S.S., Armstrong, N.R., (in preparation).
67. R. Cieslinski and N. R. Armstrong, *J. Electroanal.l Chem.*, **161**, 59 (1984).
68. Y. Ayato, A. Takatsu, K. Kato, J. H. Santos, T. Yoshida and N. Matsuda, *J. Electroanal. Chem.*, **578**, 137 (2005).
69. Y. Ayato, A. Takatsu, K. Kato and N. Matsuda, *J. Electroanal. Chem.*, **595**, 87 (2006).
70. Y. Ayato, A. Takatsu, K. Kato and N. Matsuda, *IEICE Trans. Electron.*, **E89C**, 1750 (2006).